

CFD ANALYSIS OF THE DUST LOADING IN A CYCLONE SEPARATOR FOR MILK POWDER

ANÁLISIS CFD DE LA CARGA DE POLVO EN UN SEPARADOR CICLÓN PARA LECHE EN POLVO

**Christian O. Díaz-Ovalle^{1,*}, María J. Ramírez-Rivera¹, Florianne Castillo-Borja²,
Edgar O. Castrejón-González³**

(1) Tecnológico Nacional de México/I.T. de Roque, Departamento de Ingenierías, km 8.0 carretera Celaya-Juventino Rosas, Celaya, Guanajuato, 38124, México

(2) TecNM/Instituto Tecnológico de Aguascalientes, Departamento de Ingeniería Química, Av. Adolfo López Mateos 1801 Ote., Aguascalientes, Aguascalientes, 20256, México

(3) Tecnológico Nacional de México en Celaya, Departamento de Ingeniería Química, Av. Tecnológico y Antonio García Cubas s/n, Celaya, Guanajuato, C.P. 38010, México

*Corresponding author (e-mail: christian.do@roque.tecnm.mx)

Recibido: 30/05/2023 - Evaluado: 15/06/2023 - Aceptado: 27/06/2023

ABSTRACT

Cyclone separators are relevant equipment in the food industry for collecting powder products. This equipment presents a particular flow behavior that has taken attention to improve its operative conditions and enhance the collecting efficiency. Even more, the literature indicates the effect of dust loading into the flowthrough, which has not been applied in foodstuffs. This analysis considers the dust loading effect on the hydrodynamic behavior during the milk powder collection. Computational Fluid Dynamics (CFD) technique, ANSYS FLUENT® package, applied on a Tengbergen C cyclone separator with several powder milk loading concentrations. The obtained values of the total pressure drop have indicated the influence of the dust loading concentration with a reduction of around 30% concerning the clean flow process, which coincides with the literature.

RESUMEN

Los separadores ciclones son equipos importantes en la industria de alimentos para recolectar productos en polvo. Este equipo presenta un comportamiento especial en su flujo que ha sido considerado para mejorar las condiciones de operación y la eficiencia de recolección. Inclusive, la literatura indica el efecto de la carga de polvo en el flujo interno, pero no ha sido aplicado en alimentos. Este estudio considera el efecto de la carga de polvo sobre el comportamiento hidrodinámico de la recolección de leche en polvo. La Dinámica Computacional de Fluidos, usando el software ANSYS FLUENT®, es aplicada en un ciclón tipo Tengbergen C con varias concentraciones de leche en polvo. El valor obtenido de la caída de presión total indica la influencia de la concentración de polvo en el ciclón. Los resultados indicaron una reducción de la caída de presión total cerca del 30% respecto al proceso sin polvo, lo cual coincide con la literatura.

Keywords: Computational Fluid Dynamics, pressure drop, powder product, internal flow
Palabras clave: Dinámica Computacional de Fluidos, caída de presión, producto en polvo, flujo interno

INTRODUCTION

In the last decades, powder products have characterized the food industry, and most of them come from the spray drying process (Anandharamakrishnan, 2017). The economic importance of the powder products obligates a high efficiency in its recollection, which is possible by using cyclone separators. This equipment has been studied for several decades due to its special hydrodynamic behavior (Hoffmann & Stein, 2008), which is a result of the shape and consists of: a) a tangential inlet to the cylindrical shape, b) descending pattern to a conical shape, and c) ascending flow to the inner cylindrical exit (vortex finder). The dust particles are collected through the flow, and trapped at the bottom where a rotary valve conserves the pressure drop inside. Shepherd and Lapple (1939; 1940) have provided the fundamental elements for studying cyclone separators. They concluded that the geometrical proportions regulate the fluid inside the cyclone separator, it was observed in the pressure drop, tangential, and axial velocity. From that, the analysis of cyclone separators has been greatly extended; Alex *et al.* (2022), have provided a recent bibliographical study about cyclone separators; Guo *et al.* (2024), have indicated the geometrical effect of the cyclone separators in the efficiency and performance; and Dehdarinejad and Bayareh (2021), have explained the use of modeling and simulation techniques to study them, where the CFD is the more suitable tool.

The study of cyclone separators relates experimental tests, empirical models, CFD analysis, and multi-objective optimization, such as the works by Demir (2014), Singh *et al.* (2016), Shastri *et al.* (2022), and Venkatesh *et al.* (2019), respectively. In a particular way, the effect of loaded dust is remarkable in cyclone separators, and Briggs (1946) and Smolik (1975), both cited by Cortés and Gil (2007), and Baskakov *et al.* (1990); have proposed some empirical models to modify the pressure drop value. Trefz and Muschelknautz (1993), have provided a model to predict the separation efficiency for several critical concentrations of solids by considering the friction factors. Fassani and Goldstein (2000), determined a reduction of separation efficiency with respect to the dust loading concentration. Experimentally, Gil *et al.* (2002), observed the influence of dust loading in the pressure drop by comparing the results with models from the literature. Chen and Shi (2007), applied the method for dust-laden gases to determine the pressure drop by changing the dust loading concentration, where the main factor was the intensity of gas swirling motion. Qian *et al.* (2007), applied a particle predictive model to determine the effect of the dust loading concentration on the internal flows. Wan *et al.* (2008), simulated the distribution of diverse dust loading concentrations. Chu *et al.* (2009), studied the main forces (normal, tangential, torque, and body forces) at different particle concentrations. Li *et al.* (2011), presented a set of models to modify the pressure drop at different dust loading concentrations. Hwang *et al.* (2019), developed an extended CFD study of the loading dust effect on the hydrodynamic behavior in cyclone separators, where a decreasing model modifies the pressure drop. Morin *et al.* (2021), demonstrated that collection efficiency is proportional to the dust loading concentration. All these studies have demonstrated the reduction of pressure drop in dust loading. In this work, a CFD simulation is developed to understand the level of influence of the mass flow rates of loaded dust on the internal flow. The literature does not present studies on collected foodstuffs by cyclone separators, whereby milk powder is taken into account herein.

METHODOLOGY

This analysis corresponds to a Eulerian-Lagrangian approach, where the fluid is a continuous phase, and the milk powder is a discrete phase. The CFD strategy considers: computational domain development, meshing process to discretize the geometry, boundary conditions and governing equations declaration, and numerical solution. The software ANSYS® Fluent 2024 R1 provided the tools to develop this study. The next sections include these steps to analyze the effect of particle loading in a cyclone separator.

Description of the system

The literature reports a set of cyclone separators with different shapes and sizes. Gamiño-Tovar *et al.* (2018), have recommended the Tengbergen C cyclone separator for milk powder. Figure 1 a) contains the dimensions of

this equipment based on a diameter of 1.2 m. Moreover, the air is considered ideal gas and gets into the cyclone separator at 1 kg/s with a dynamic viscosity of 2.14×10^{-5} kg/(ms). The milk powder enters at 10 m/s with a density of 500 kg/m^3 and an average particle diameter (d_{ave}) of $5 \mu\text{m}$ (Onwulata, 2006), which is distributed in 10 different diameters for $1 \mu\text{m} \leq d \leq 10 \mu\text{m}$ in the Rosin-Rammler distribution: $x_i = \exp(-d/d_{ave})^n$, where x is the mass fraction of a particle of diameter d and n is the spread parameter with the standard value of 3.5.

Governing equations and boundary conditions

The mass and momentum conservation equations model the internal flow of a cyclone separator. The nature of the twist design demands the modeling of turbulence. For the case of cyclone separators, the literature has proposed the Reynolds-Stress Model (Dehdarinejad & Bayareh, 2021) due to its robustness. Nevertheless, the κ - κ_L - ω model is a novel option to predict the tangential flow inside a cyclone separator. This model is a short approach to turbulence that applies in the transition between laminar and turbulence flows, predicts the development of the boundary layer, and calculates transition onset. The transition prediction involves the kinetic energy for the turbulent and laminar regions, κ and κ_L , respectively, which computes the laminar and turbulent fluctuations and approximates the turbulent large-scale energy (Walters & Cokljat, 2008). Table 1 contains the governing equation for this study.

Table 1: Governing equation for this study.

Description	Equation
Mass conservation	$\nabla \cdot \rho \mathbf{v} = 0$
Momentum conservation	$\nabla \cdot \rho \mathbf{v} \mathbf{v} = -\nabla p + \nabla \cdot \boldsymbol{\tau} + \rho \mathbf{g} + \mathbf{F}$
Turbulence kinetic energy	$\nabla \cdot \mathbf{v} k_T = P_{KT} + R + R_{NAT} - \omega k_T - D_T + \nabla \cdot \left[\left(\mathbf{v} + \frac{\mathbf{a}_T}{a_k} \right) \nabla k_T \right]$
Laminar kinetic energy	$\nabla \cdot \mathbf{v} k_L = P_{KL} - R - R_{NAT} - D_T + \nabla \cdot [v \nabla k_L]$
Inverse turbulent time-scale	$\nabla \cdot \mathbf{v} \omega = C_{\omega 1} \frac{\omega}{k_T} P_{KT} + \left(\frac{C_{\omega R}}{f_W} - 1 \right) (R + R_{NAT}) \frac{\omega}{k_T} - C_{\omega 2} \omega^2 + C_{\omega 3} a_T f_W^2 \frac{\sqrt{k_T}}{d^3} + \nabla \cdot \left[\left(\mathbf{v} + \frac{\mathbf{a}_T}{a_\omega} \right) \nabla \omega \right]$
Nomenclature: D_T, D_L : near-wall dissipation terms, \mathbf{g} : vector form of gravity acceleration, \mathbf{F} : gas-particle interactive force, k_L and k_T laminar and turbulent kinetic energy, respectively, P_{KT} : production term, P_{KL} : production of laminar kinetic energy, R : averaged effect of the breakdown of streamwise fluctuations into turbulence, R_{NAT} : breakdown of turbulence due to instabilities, \mathbf{v} : velocity vector, ν : kinematic viscosity, a_T : turbulent scalar diffusivity, ρ : density, $\boldsymbol{\tau}$: shear strength, ω : inverse turbulent time-scale, d, f_W : parameters, and $a_\omega, a_k, C_{\omega 1}, C_{\omega 2}, C_{\omega 3}, C_{\omega R}$: constants.	

The particle motion in cyclone separators take into account the body, fluid drag, buoyance forces, and gas-particle interactive force (Clift *et al.*, 1978; Hoffmann & Stein, 2008; Lapple & Shepherd, 1940; Yeoh & Tu, 2010). Thus, the representative model corresponds to:

$$\frac{d\mathbf{v}_{S,i}}{dt} = \frac{g(\rho_s - \rho)}{\rho_s} + C_{D,i} \frac{3\rho(\mathbf{v} - \mathbf{v}_{S,i})|\mathbf{v} - \mathbf{v}_{S,i}|}{4d_{ave,i}\rho_s} - \frac{\mathbf{F}}{\rho_s} \tag{1}$$

Morsi and Alexander (1972), developed a spherical drag model to approximate the $C_{D,i}$, such as Table 2 indicates with $Re_{S,i} = |\mathbf{v} - \mathbf{v}_{S,i}| \rho d_{ave,i} (\mu)^{-1}$.

Table 2: Spherical drag model by Morsi and Alexander.

Reynolds number range	$1 < Re_{S,i} \leq 10$	$10 < Re_{S,i} \leq 100$	$100 < Re_{S,i} \leq 1000$
Model for $C_{D,i}$	$1.222 + \frac{29.1667}{Re_{S,i}} - \frac{3.8889}{(Re_{S,i})^2}$	$0.6167 + \frac{46.5}{Re_{S,i}} - \frac{116.67}{(Re_{S,i})^2}$	$0.3644 + \frac{98.33}{Re_{S,i}} - \frac{2778}{(Re_{S,i})^2}$

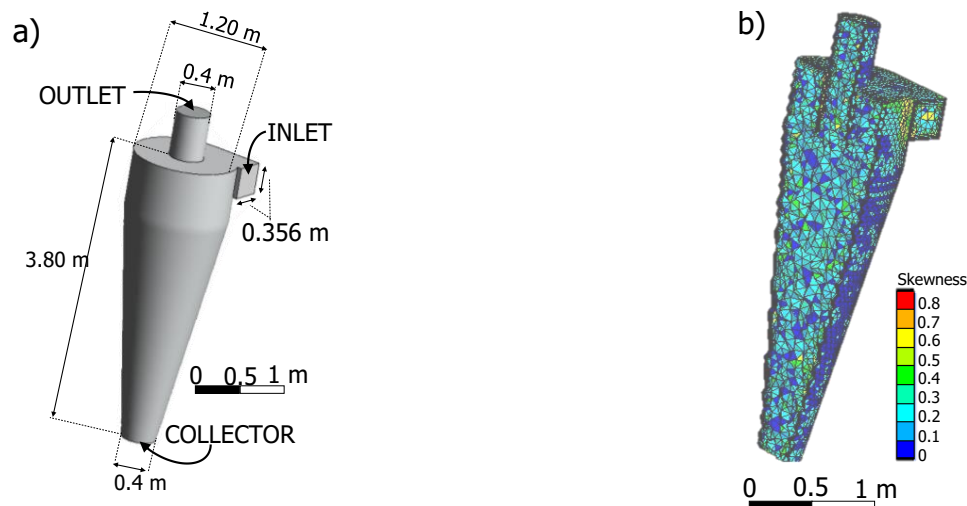


Fig. 1: Representation of the Tengbergen C cyclone separator: a) size details and boundary conditions, and b) meshing.

Figure 1 b) schematizes the boundary conditions: inlet, outlet, and collector. The collector element is a closed boundary (wall) due to the rotary valve effect that maintains the pressure drop (Hoffmann & Stein, 2008; Westergaard, 2004). The inlet boundary considers a mass flow rate (1 kg/s), and the outlet boundary performs the mass conservation to guarantee the inlet mass flow rate. Under this assumption, the simulation computes the pressure drop due to the inlet and outlet boundaries dispensing with the pressure value. The remaining faces inside are no-slip wall boundaries. The inlet, outlet, and collector boundaries follow the particle effects reflect, escape, and trap, respectively. The boundary conditions considered the turbulent intensity of 5% that approximates the relation $\sqrt{(\sum v_i'^2)}/\bar{v}_i$. Finally, the particles flow in the cyclone separator as a homogeneous surface distribution from the inlet boundary.

Numerical solution

The meshing development was possible with ANSYS Meshing ®. The treatment provided 90,742 tetrahedron cells around 5.7 cm with a skewness average of 0.226. The former parameter describes the mesh quality based on the non-optimal cells with deformed proportions, and the desired value is close to 0 and indicates perfect hexahedron cells. Figure 1 b) shows the developed mesh where the worst cells are close to the vortex finder (upper exit duct). On the other hand, the solution of the particles used a time step of 0.5 s with two-time steps applied for each 20 fluid iterations. For this steady-state scenario, the solution considers the two-way coupling principle and the high-order trapezoid scheme. For the fluid, the numerical solution followed the SIMPLE algorithm, which is the conventional algorithm for this flow. The second-order upwind approach interpolated the cell values. The initialization procedure took the values from the inlet. The simulations required an average of 40 min to solve 3,000 iterations in a computer with 24 GB RAM Intel ® Core™ i7-3770 3.4 GHz processor. The nature of the problem did not demand a high computation level, whereby the solver process was one without the use of GPUs.

RESULTS

The analysis compares the scenarios with and without the loading of particles. The case without loading of particles is called clean flow. Both results included the hydrodynamic behavior to guarantee an acceptable cyclone performance based on the literature and the pressure drop calculation (total pressure difference between the inlet and the outlet boundaries). In addition, the analysis considered the milk powder loading concentrations (g/m^3): 12.25, 29, 61.25, and 122.5, which correspond to the particle mass flow rates (g/s): 10, 25, 50, and 100, respectively. The simulation with particles included the distribution inside the cyclone and the fitting to existent models to indicate the influence of the particle loading concentration on the total pressure drop.

Hydrodynamic behavior

Figure 3 depicts the main flow parameters of a cyclone separator: velocity (streamlines), total pressure, tangential velocity, and axial velocity profiles. All these responses coincide with the literature descriptions, such as Hoffmann and Stein (2008), and Cortés and Gil (2007). The clean flow simulation reaches low pressure profile values, $-40 \text{ Pa} < P < 10 \text{ Pa}$, with a narrow suction region in the core. The velocity streamlines describe the expected behavior for a cyclone: tangential inlet flow, descendent flow by reduction (conical shape), and ascendent flow through the vortex finder. The tangential velocity depicts the Rankine vortex with a maximum value in the core of the cylindrical region, which indicates the distribution of the kinetic energy flow through. Finally, the axial velocity presents the descendent direction of the flow (negative values) close the walls and the ascendent direction (positive values) at the cyclone core. All the cases of dust loading yield similar values between them. In contrast to the clean simulation, the pressure profile reaches a wide suction region at the cyclone core; the velocity presents an acceleration zone on the walls; and the tangential velocity decreases close to the walls.

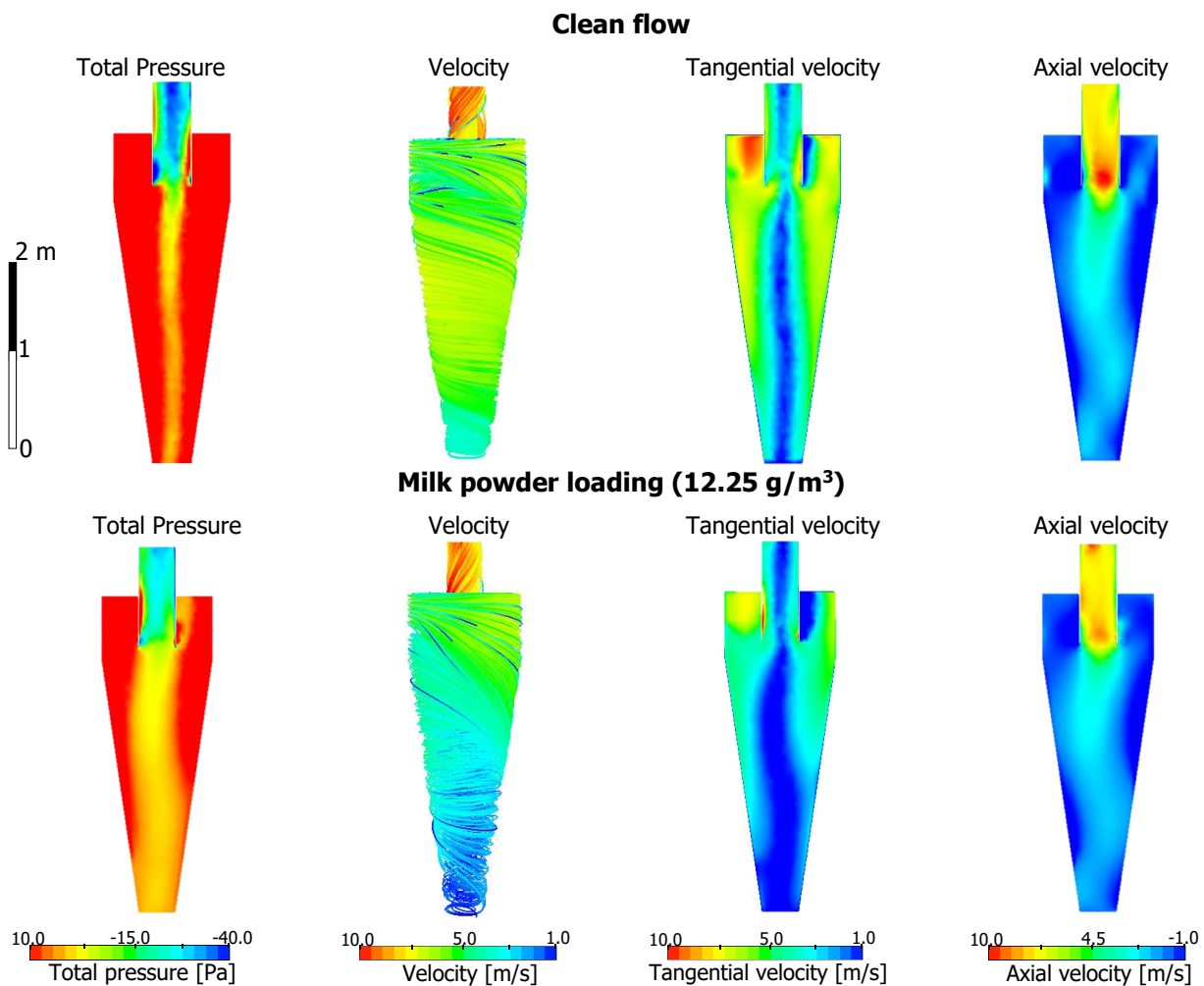


Fig. 3: Hydrodynamic behavior of the cyclone separator in a central plane, clean flow and milk powder loading (12.25 g/m^3).

Pressure drop

The pressure drop (ΔP) refers to the losses of kinetic energy upon the walls. The literature presents theoretical approaches to compute ΔP , such as Barth model, Demir model, etc. (Demir, 2014). Nevertheless, the use of CFD

is a suitable option to determine ΔP ; herein, the clean flow simulation obtained $\Delta P=107.62$ Pa, which is different from the models: First (590.5 Pa), Stairmand (345.6 Pa), Chen and Shi (353.2 Pa) and Demir (351.1 Pa). The difference indicates the underprediction by CFD, which might be validated only by experimental data. Although to present this difference, the CFD simulation rigorously evaluates the mass, momentum, and energy conservation equations that represent valid assumptions by including the turbulence phenomenon. The loading dust reduces the values of ΔP . Table 2 contains the ΔP values for the proposed dust loading concentration, and these values are a 30% reduction of ΔP from the clean flow simulation that corresponds to the indicated by Hoffmann and Stein (2008), and Fassani and Goldstein (2000) experimentally predicted a reduction of 47% for the pressure drop. Cortés and Gil (2007), Gil *et al.* (2002), and Hoffmann and Stein (2008) have summarized correction models for ΔP such as the Briggs model, Smolik model, and Baskakov model, who suggested correcting to $\Delta P=\Delta P_{\text{clean}}\xi$, where ξ is the pressure drop correction factor in response to the dust loading concentration, C . A nonlinear root square method was developed in MS Excel® using the Solver® tool to fit the data into the corrections models from the literature. Table 3 contains the correlation parameters and Pearson's parameter, R^2 . All models observed similar values of R^2 .

Table 2: Pressure drop values at different values of dust loading concentration

ΔP (Pa)	107.62	68.90	68.54	67.56	67.40
C (g/m ³)	0	12.25	29	61.25	122.5

Table 3: Fitting to correction models.

Model	$\xi = (a_1 + a_2 C^{a_3})^{a_4} + a_5 C$		
Parameters	Briggs model	Smolik model	Baskakov model
a_1	1	1	1
a_2	0.5283	-0.3460	0.5247
a_3	0.0286	0.0181	0.0319
a_4	-1	1	-1
a_5	0	0	2.62×10^{-5}
R^2	0.92052	0.92053	0.92193

The particle tracking presents differences between the dust loading cases. The case of 12.25 g/m³ of milk powder distributed the particles in the conical zone, which helps to collect the milk powder. The increment of the dust loading concentration yielded a homogeneous distribution of the milk powder into the cyclone separator. The case of 122.5 g/m³ of milk powder presented the existence of particles at the cyclone upper wall and through the vortex finder. Thus, this increment of particles inside reduced the existence of milk powder at the collector, which is related to the distribution of the kinetic energy upon the milk powder. Figure 4 contains the comparison of the four cases of particle loading.

CONCLUSIONS

The application of CFD in cyclone separators is recurrent for analyzing the hydrodynamic and particle tracking. Herein, this computational technique has provided an understanding of the dust loading on the cyclone separator performance. In principle, the pressure drop is reduced by 30% (similar to experimental results), and the total pressure, tangential velocity, and axial velocity profiles change at a low level in response to milk powder loading concentration. The dust loading is inverse to the dust recovery which remarks an operation limit in the cyclone separator design. In such a case, the literature recommends a serial cyclone separator.

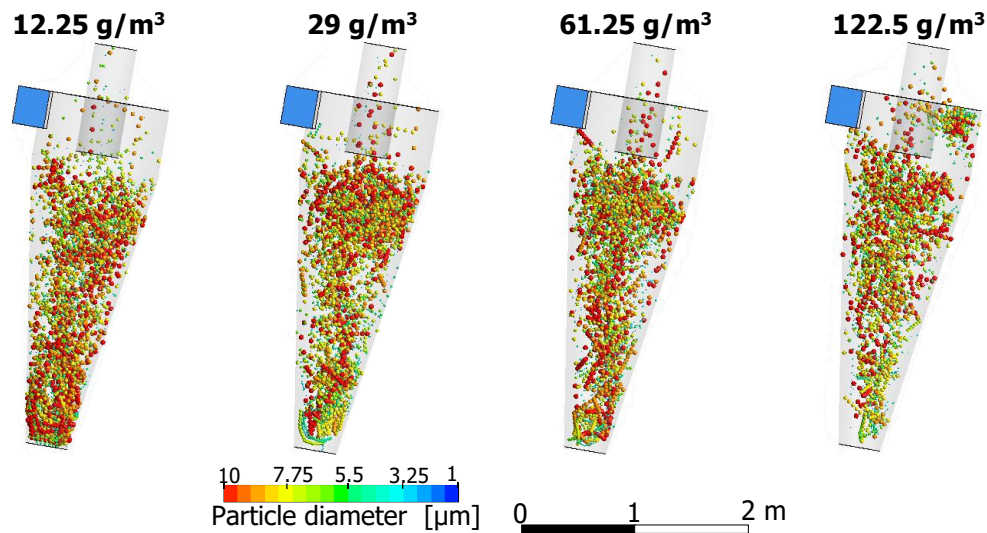


Fig. 4. Particle distribution in the cyclone separator of milk powder.

NOMENCLATURE

a_k	parameters for the pressure drop correction
C	dust loading concentration
C_{Di}	spherical drag coefficient
d_{ave}	average particle diameter
d	particle of diameter
\mathbf{F}	gas-particle interactive force
\mathbf{g}	vector form of gravity acceleration
p	pressure
$Re_{s,i}$	Reynolds number
v'_i	velocity fluctuation of the i component
\bar{v}_i	velocity average value of the i component
\mathbf{v}	velocity of the fluid
$\mathbf{v}_{s,i}$	velocity vector of the solid particle
x_i	mass fraction of a particle

Greek letters

ΔP	pressure drop
ΔP_{clean}	pressure drop in a flow without particles
κ	kinetic energy for the turbulent region
κ_L	kinetic energy for the laminar region
μ	viscosity of the fluid
ξ	pressure drop correction factor
ρ	density of the fluid
ρ_s	density of the solid particle
ω	Inverse turbulent time-scale

Acronyms

CFD	Computational Fluid Dynamics
SIMPLE	Semi-Implicit Method for Pressure Linked equations

ACKNOWLEDGEMENT

The authors appreciate the financial support by CONAHCYT, México.

REFERENCES

- Alex, F.J., Tan, G., Agyeman, P.K., Ansah, P.O., Olayode, I.O., Fayzullayevich, J.V., *et al.* (2022). Bibliometric Network Analysis of Trends in Cyclone Separator Research: Research Gaps and Future Direction. *Sustainability*, *14* (22), 14753.
- Anandharamakrishnan, C. (2017). *Handbook of Drying for Dairy Products*. Wiley and Sons.
- Baskakov, A.P., Dolgov, V.N. & Goldobin, Y.M. (1990). Aerodynamics and heat transfer in cyclones with particle-laden gas flow. *Experimental Thermal and Fluid Science*, *3* (6), 597-602.
- Chen, J. & Shi, M. (2007). A universal model to calculate cyclone pressure drop. *Powder Technology*, *171* (3), 184-191.
- Chu, K.W., Wang, B., Yu, A.B. & Vince, A. (2009). CFD-DEM modelling of multiphase flow in dense medium cyclones. *Powder Technology*, *193* (3), 235-247.
- Clift, R., Grace, J.R. & Weber, M.E. (1978). *Bubbles, drops, and particles*. Dover Publications, Inc.
- Cortés, C. & Gil, A. (2007). Modeling the gas and particle flow inside cyclone separators. *Progress in Energy and Combustion Science*, *33* (5), 409-452.
- Dehdarinejad, E. & Bayareh, M. (2021). An Overview of Numerical Simulations on Gas-Solid Cyclone Separators with Tangential Inlet. *ChemBioEng Reviews*, *8* (4), 375-391.
- Demir, S. (2014). A practical model for estimating pressure drop in cyclone separators: An experimental study. *Powder Technology*, *268* (0), 329-338.
- Fassani, F.L.s. & Goldstein, L. (2000). A study of the effect of high inlet solids loading on a cyclone separator pressure drop and collection efficiency. *Powder Technology*, *107* (1), 60-65.
- Gamiño-Tovar, M.S., Castillo-Borja, F., Vázquez-Román, R., Díaz-Ovalle, C.O., Guzmán-Zazueta, A. & Herrera-Enciso, F. (2018). Análisis del efecto geométrico de ciclones en el secado por aspersión de leche usando CFD [Analysis of the geometric effect of cyclone separators over spray-dryer process of milk using CFD]. *Avances en Ciencias e Ingeniería*, *9* (1), 11-23.
- Gil, A., Romeo, L.M. & Cortés, C. (2002). Effect of the Solid Loading on a PFBC Cyclone with Pneumatic Extraction of Solids. *Chemical Engineering & Technology*, *25* (4), 407-415.
- Guo, M., Yang, L., Son, H., Le, D.K., Manickam, S., Sun, X., *et al.* (2024). An overview of novel geometrical modifications and optimizations of gas-particle cyclone separators. *Separation and Purification Technology*, *329*, 125136.
- Hoffmann, A.C. & Stein, L.E. (2008). *Gas cyclones and swirl tubes. Principles, design and operation*. Springer-Verlag Berlin Heidelberg.

- Hwang, I.S., Jeong, H.J. & Hwang, J. (2019). Numerical simulation of a dense flow cyclone using the kinetic theory of granular flow in a dense discrete phase model. *Powder Technology*, 356, 129-138.
- Lapple, C.E. & Shepherd, C.B. (1940). Calculation of particle trajectories. *Industrial and Engineering Chemistry*, 32 (5), 605-617.
- Li, S., Yang, H., Wu, Y. & Zhang, H. (2011). An Improved Cyclone Pressure Drop Model at High Inlet Solid Concentrations. *Chemical Engineering & Technology*, 34 (9), 1507-1513.
- Morin, M., Raynal, L., Karri, S.B.R. & Cocco, R. (2021). Effect of solid loading and inlet aspect ratio on cyclone efficiency and pressure drop: Experimental study and CFD simulations. *Powder Technology*, 377, 174-185.
- Morsi, S.A. & Alexander, A.J. (1972). An investigation of particle trajectories in two-phase flow systems. *J. Fluid Mechanics*, 55 (2), 193-208.
- Onwulata, C., ed. (2006). *Encapsulated and powdered foods*. Taylor & Francis Group, Boca Raton, US.
- Qian, F., Huang, Z., Chen, G. & Zhang, M. (2007). Numerical study of the separation characteristics in a cyclone of different inlet particle concentrations. *Computers & Chemical Engineering*, 31 (9), 1111-1122.
- Shastri, R., Sharma, R.P. & Brar, L.S. (2022). Numerical investigations of cyclone separators with different cylinder-to-cone ratios. *Particulate Science and Technology*, 40 (3), 337-345.
- Shepherd, C.B. & Lapple, C.E. (1939). Flow Pattern and Pressure Drop in Cyclone Dust Collectors. *Industrial & Engineering Chemistry*, 31 (8), 972-984.
- Shepherd, C.B. & Lapple, C.E. (1940). Flow Pattern and Pressure Drop in Cyclone Dust Collectors Cyclone without Intel Vane. *Industrial & Engineering Chemistry*, 32 (9), 1246-1248.
- Singh, P., Couckuyt, I., Elsayed, K., Deschrijver, D. & Dhaene, T. (2016). Shape optimization of a cyclone separator using multi-objective surrogate-based optimization. *Applied Mathematical Modelling*, 40 (5), 4248-4259.
- Trefz, M. & Muschelkautz, E. (1993). Extended cyclone theory for gas flows with high solids concentrations. *Chemical Engineering & Technology*, 16 (3), 153-160.
- Venkatesh, S., Sakthivel, M., Avinasilingam, M., Gopalsamy, S., Arulkumar, E. & Devarajan, H.P. (2019). Optimization and experimental investigation in bottom inlet cyclone separator for performance analysis. *Korean Journal of Chemical Engineering*, 36 (6), 929-941.
- Walters, D.K. & Cokljat, D. (2008). A Three-Equation Eddy-Viscosity Model for Reynolds-Averaged Navier–Stokes Simulations of Transitional Flow. *Journal of Fluids Engineering*, 130 (12), 121401. <https://doi.org/10.1115/1.2979230>
- Wan, G., Sun, G., Xue, X. & Shi, M. (2008). Solids concentration simulation of different size particles in a cyclone separator. *Powder Technology*, 183 (1), 94-104.
- Westergaard, V. (2004). *Tecnología de la leche en polvo. Evaporación y secado por atomización*. Niro A/S, Copenhagen.
- Yeoh, G.-H. & Tu, J. (2010). *Computational techniques for multi-phase flows*. Butterworth-Heinemann.

